

Viscoelastic Fluid and Dean Flow Effects on Flow and Heat Transfer Characteristics of Serpentine Channel

Kazuya Tatsumi ^{*,§}, Yousuke Tanaka ^{*}, Reiko Kuriyama ^{*} and Kazuyoshi Nakabe ^{*}

^{*} Department of Mechanical Engineering and Science, Kyoto University, Kyoto, Japan

[§]Correspondence author. Fax: +81 75 383 3608 Email: tatsumi@me.kyoto-u.ac.jp

ABSTRACT Viscoelastic fluid can increase the heat transfer coefficient of the low Reynolds number flow in the serpentine channel by generating unsteady and secondary flows. A pair of longitudinal vortices which is similar in form to Dean vortices is generated mainly due to the first normal stress differences. These vortices carry the low temperature fluid toward the channel sidewalls and increase the heat transfer coefficient. However, each contribution of the viscoelastic effect and the centrifugal force (Dean vortices) on the secondary flow and heat transfer characteristics are not clearly investigated and distinguished, especially in the case of serpentine channel. In this study, we conducted three-dimensional numerical computation on viscoelastic fluid in serpentine channel using Oldroyd model. The effects of the Reynolds number (Dean number) and Weissenberg number on the flow structure and heat transfer coefficients were evaluated. In the results, the viscoelastic flow and Dean flow gave certain similar aspects. However, the viscoelastic fluid generated stronger secondary flows and producing higher heat transfer coefficient for high Weissenberg number conditions. Further, we showed that the first normal stress difference plays an important role to characterize the flow, and good agreement can be obtained between the measurement and computation by introducing the dimensionless normal stress difference.

INTRODUCTION

Viscoelastic fluid is a non-Newtonian fluid that exhibits elastic properties in addition to viscosity. The elasticity will produce normal stresses in the flow, when shear and stress are applied to the fluid. This force changes the main flow structure, generates secondary flows, and increases the flow instability. The unsteady and secondary flows enhance the fluid mixing and heat transfer, and therefore, studies on viscoelastic fluids in various types of channels have been made by many researchers. Among these, channel with curvature is known to produce longitudinal vortex-like secondary flow similar to Dean vortex due to the normal stress differences of the viscoelastic fluid [e.g., Joo et al. 1994, Norouzi et al. 2009, Helin et al. 2009]. These vortices also appears in the serpentine channel, and furthermore, the inflection point of the curvatures increases the strength of the radial flow and the flow instability [Burghelea et al. 2004, Tatsumi et al., 2011, Zilz et al. 2012]. Thus, the heat transfer coefficient increases especially at the outer sidewalls of the serpentine channel [Tatsumi et al., 2014, Abed et al. 2016, Tatsumi et al. 2019]. The flow in these channels is a mixture of the viscoelastic fluid flow and the Dean vortices. However, the difference between the contribution of the two flow on the heat transfer characteristics, and moreover, the combined effects are not clearly evaluated. In this study, we conducted a three-dimensional computation on flow and temperature fields of the viscoelastic fluid in serpentine channel and discussed the effect of the Dean vortices and the viscoelastic fluid on the flow and heat transfer characteristics varying the Reynolds number and Weissenberg number. We will first present the

Table 1 Fluid properties and conditions of the computation and experiment

	Viscosity μ_0 [Pa·s]	Relaxation time λ [s]	Re	N_D	Wi	Pr	N_1^*
Computation	0.53	0.056	0.5-28	0.28-16	0.5-6	3.2×10^3	6.5-234
Measurement	0.28	3.73	1.0-2.1	0.57-1.2	6.0	3.2×10^3	6.4-260

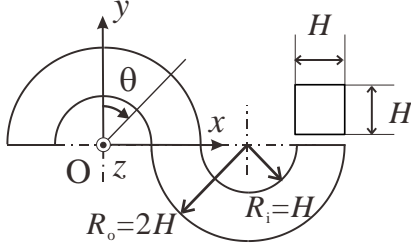


Figure 1 Computational domain.

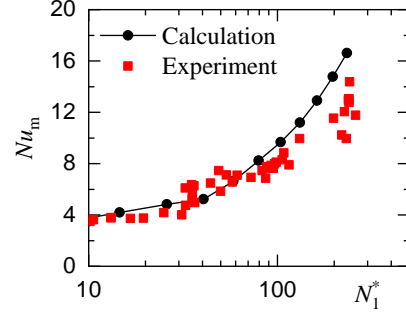


Figure 2 Nusselt number and dimensionless normal stress differences N_1^* .

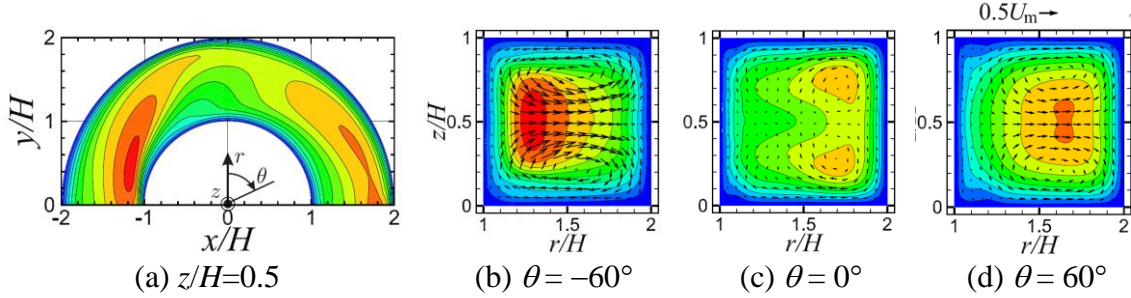


Figure 3 Contours of the streamwise velocity u_θ and velocity vectors on the r - z and r - θ planes.

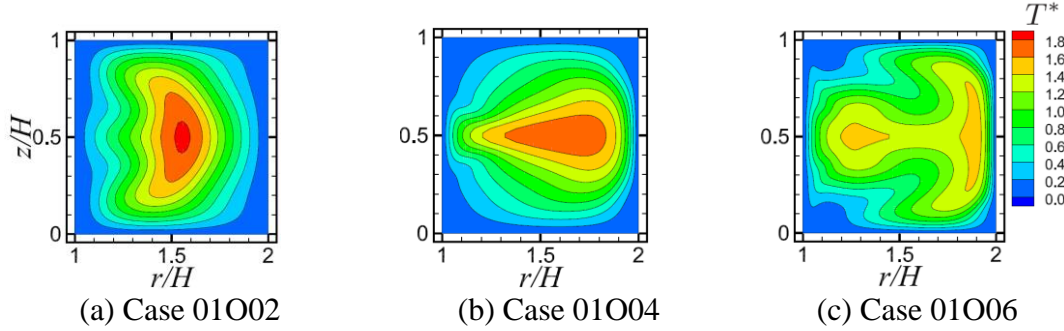


Figure 4 Contour of the dimensionless temperature T^* on the r - z plane at $\theta = -60^\circ$.

comparison of the numerical results with the measurements for validation. The dimensionless value of the first normal stress difference is introduced here to adjust the conditions of the computation and measurement. The effects of the Dean flow and fluid viscoelasticity on the flow and heat transfer coefficients will, then, be presented; the flow structure and Nusselt number distribution along the curved channel is compared, and how the combined effect can increase the heat transfer performance are shown.

METHODS

Numerical Procedure Unsteady and three-dimensional form of the continuous equation, Navier-Stokes equation, and energy conservation equation are solved in the present computation. These equations are discretized by applying the QUICK scheme to the convection terms and 4th order central difference scheme to the diffusion terms. The pressure term was solved using the SIMPLE algorithm. The viscoelasticity of the fluid is applied to the computation by employing the Oldroyd-B model as the constitutive equation and adding the additional stress term to the Navier-Stokes equation. Oldroyd-B

model is a fundamental model derived by also considering the behaviour of the viscoelasticity in molecular level. We used this model in order to simplify the problem which is discussed and compare with the measurements. The constitutive equation was discretized by applying 1st order upwind scheme to the convection term, and 2nd order central difference scheme to other derivatives.

Computational domain and conditions Fig. 1 (a) shows the computational domain. The serpentine channel consists of two semi-circular parts with curvature of opposite direction. The channel has a square cross section of 5 mm ($=H$) on side, and the inner and outer radii of the semicircle part are $R_i/H = 1$ and $R_o/H = 2$, respectively. Non-slip and constant temperature conditions are applied to the channel walls. Periodic boundary condition is applied to the streamwise boundaries. The fluid properties and dimensionless parameters of the computation are shown in Table 1. Grid dependency test was carried out using grid density of $42 \times 124 \times 42$, $82 \times 239 \times 82$ and $164 \times 479 \times 164$. The variation of the average heat transfer coefficient among these conditions were 12.3% and 2.95%, and of the pressure loss were 2.71% and 0.974%, respectively. Therefore, we chose the grid density of $82 \times 239 \times 82$ in the main computation.

RESULTS and DISCUSSION

Comparison with measurement The average Nusselt number Nu_m is compared with the authors' measurement [Tatsumi et al., 2014] for validation. The condition of the computation and measurement are shown in Table 1. The Reynolds number Re of the experiment and computation are similar while the Weissenberg number Wi differs largely. This is due to the difference in the relaxation time λ . Therefore, we will introduce another dimensionless parameter related to the normal stress. The term expressed as $(\tau_{\theta\theta} - \tau_{rr})/r$, which appears in the equation of motion of the radial direction as the normal stress difference N_1 , plays an important role in the generation of the secondary flow by producing force in the radial direction near the top and bottom walls and driving the fluid toward the central direction of the curvature. We can derive the following dimensionless parameter by normalizing the equation of motion applying H and the streamwise mean velocity U_m as the characteristic length and velocity.

$$N_1^* = \frac{\rho H^2}{\mu_0^2} N_1 \quad (1)$$

We will rearrange the relationship of the Nu_m with the Reynolds number or Weissenberg number to the the dimensionless first normal stress difference N_1^* as shown in Fig. 2. The results of the computation and measurement show a reasonable agreement, which indicates the validity of the present computation and that N_1^* can be an important index to represent the flow and heat transfer characteristics. Difference between the computation and measurement is found in the region of large N_1^* . This can be attributed to the shear-thinning effect of the fluid in the experiment, which decreases the normal stress in the near-wall region significantly compared to the effect on the Reynolds number and viscosity in Eq. (1).

We now show some of the computational results which represent the viscoelastic effect on the flow and temperature field of the serpentine channel. Fig. 3 shows the streamwise velocity u_θ distributions on the $r-\theta$ plane of $z/H=0.5$, and $r-z$ planes of $\theta=-60^\circ$, 0° and 60° in the case of high Weissenberg number and Reynolds number condition; $Wi=5.0$ ($N_1^*=908$) and $Re=28$. Fig. 4 shows the dimensionless temperature $T^*=(T-T_w)/(T_b-T_w)$ at $\theta=60^\circ$ for the cases of $Wi=2.0, 4.0$ and 6.0 where Re is constant as $Re=1.0$.

In Fig. 2, Nu_m is constant at low N_1^* showing the steady state and small secondary flow. As N_1^* increases, Nu_m increases due to the generation of pair of longitudinal vortex like secondary flows. Generation of these vortices can be observed clearly in the velocity distribution shown in Fig. 3 (b) and (d). The flow core region of low temperature is carried toward the outer sidewall, and enhance the heat transfer especially at the outer wall. The secondary flow is generated by the normal stress difference which gives a large value near the top and bottom wall due to the high shear stress of the flow. Therefore, the strength of the secondary flow increases as Wi (or N_1^*) increases, and the low temperature region largely moves in the spanwise and height directions of the channel as shown in Fig. 4.

Similar trend was observed in the Dean flow case (Newtonian fluid); Nu increased at the outer wall for large Dean number flow. However, the Dean vortices developed in the curve channel and converges to that of circular channel. Therefore, the heat transfer coefficient gradually increased at the outer wall along the channel. On the other hand, in viscoelastic fluid flows, the location of the high velocity region not only affected the centrifugal force, but also the normal stress difference mentioned above. The force generated at the outer wall and the top-bottom walls locally generates a secondary flow which moves the fluid of high velocity first toward the top-bottom walls and then back to the center of the cross-section. This produced the redevelopment effect in the thermal boundary layer. Further, a strong flow crossing the channel in the spanwise direction in the downstream region of the inflection point of the serpentine channel ($\theta = -60^\circ$) was generated in the viscoelastic fluid case. Thus, the viscoelasticity enhanced the heat transfer by increasing the strength of the secondary flow, and also by keeping the low temperature fluid region sweep the channel walls. Detail of these effects in relation to the Wi , Re , and N_1^* will be shown in the presentation, especially focusing on the difference of the viscoelastic fluid and Dean flow.

CONCLUSION

The flow and heat transfer characteristics of viscoelastic fluid in serpentine channel was numerically investigated in this study. We have shown that the velocity distribution and the average Nusselt number agrees well with the measurements especially when considering the dimensionless normal stress differences. Further, the independent and combined effects of the Dean vortex and the fluid viscoelasticity will be evaluated in the presentation by mapping the characteristics against the Reynolds number (Dean number) and Weissenberg number. Viscoelastic effect can increase the strength of the secondary flow, and furthermore, enhance the movement of the flow core region which leads to the redevelopment of the thermal boundary layer and further increase of the overall heat transfer coefficient.

REFERENCES

- Joo, Y. L., Shaqfeh, E. S. G. [1994], Observation of Purely Elastic Instabilities in the Taylor-Dean Flow of a Boger Fluid, *J. Fluid Mech.*, Vol. 262, pp. 27-73.
- Helin, L., Thais, L., Mompean, G. [2009], Numerical Simulation of Viscoelastic Dean Vortices in a Curved Duct, *J. Non-Newtonian Fluid Mech.*, Vol. 156, pp. 84-94.
- Norouzi, M., Kayhani, M. H., Nobari, M. R. H., Karimi-Demneh, M. [2009], Convective Heat Transfer of Viscoelastic Flow in a Curved Duct, *World Academy of Sci., Eng. and Tech.*, Vol. 56, pp. 327-333.
- Burghilea, T., Segre, E., Bar-Joseph, I., Groisman, A., Steinberg, V. [2004], Chaotic Flow and Efficient Mixing in a Microchannel with Polymer Solutions, *Physical Review E*, Vol. 69, p. 0066305.
- Tatsumi, K., Takeda, Y., Suga, K., Nakabe, K. [2011], Turbulence Characteristics and Mixing Performance of Viscoelastic Fluid Flow in a Serpentine Microchannel, *J. Physics Conference Series*, Vol. 318, p. 092020.
- Tatsumi, K., Nagasaka, W., Matsuo, T., Nakabe, K., A Numerical and Experimental Study on Flow and Heat Transfer Characteristics of Viscoelastic Fluid in a Serpentine Channel, *Proc. of the 15th International Heat Transfer Conference IHTC15-9615* 1-14.
- Zilz, J., Poole, R. J., Alves, M. A., Bartolo, D., Levaché, B., Lindner, A. [2012], Geometric Scaling of a Purely Elastic Flow Instability in Serpentine Channels, *J. Fluid Mech.*, Vol. 712, pp. 203-218.
- Abed, W. M., Whalley, R. D., Dennis, D. J. C., Poole, R. J. [2016], Experimental Investigation of the Impact of Elastic Turbulence on Heat Transfer in a Serpentine Channel, *J. Non-Newtonian Fluid Mech.*, Vol. 231, pp. 68-78.
- Tatsumi, K., Nagasaka, W., Kimura, R., Shinotsuka, N., Kuriyama, R., Nakabe [2019], Local Flow and Heat Transfer Characteristics of Viscoelastic Fluid in a Serpentine Channel, *Int. J. Heat Mass Transfer*, Vol. 138, pp. 432-442.
- Boger, D. V., Mackay, M. E. [1991], Continuum and Molecular Interpretation of Ideal Elastic Fluids, *J. Non-Newtonian Fluid Mech.*, Vol. 41, pp. 133-150.
- Jomha, A. I., Reynolds, P. A. [1993], An Experimental Study of the First Normal Stress Difference – Shear Stress Relationship in Simple Shear Flow for Concentrated Shear Thickening Suspensions, *Rheologica Acta*, Vol. 32, pp. 457-464.